

## Structural effects on the calculated semiconductor gap of CrSi<sub>2</sub>

L. F. Mattheiss

*AT&T Bell Laboratories, Murray Hill, New Jersey 07974*

(Received 16 October 1990)

The results of band calculations for hexagonal CrSi<sub>2</sub>, carried out in the local-density approximation, predict an indirect semiconductor gap of 0.30 eV which is in excellent agreement with the measured optical value ( $\sim 0.35$  eV). The calculated gap, which occurs within the Cr 3*d* manifold, is particularly sensitive to the local Cr-Si coordination geometry. It decreases with uniaxial pressure along *c* and vanishes for the alternative sequencing of hexagonal-type CrSi<sub>2</sub> layers that characterize the orthorhombic and tetragonal phases of the refractory (groups IV–VI) transition-metal disilicides.

Transition-metal silicides have received increased attention in recent years because of their practical importance in silicon-based microelectronics as Schottky barriers and low-resistivity interconnects.<sup>1,2</sup> The refractory disilicides *RSi<sub>2</sub>* (i.e., those containing groups IV–VI transition-metal elements *R*) are especially attractive in such applications because of their high-temperature stability and generally low electrical resistivities. Unlike their cubic group-VIII counterparts CoSi<sub>2</sub> and NiSi<sub>2</sub>, the refractory disilicides *RSi<sub>2</sub>* form with a variety of complicated, low-symmetry orthorhombic, hexagonal, and tetragonal structures. Despite their apparent diversity, these phases share a common structural element, namely, nearly hexagonal *RSi<sub>2</sub>* layers.<sup>3</sup> These compounds also share similar electronic properties<sup>4</sup> (i.e., partially filled *d* bands near  $E_F$ ), which presumably account for their novel structural and thermal properties.

Although most transition-metal silicides are metallic, a few compounds have been characterized as semiconductors, with typical band gaps in the (0.1–0.9)-eV range.<sup>2</sup> Among these semiconductors, the refractory compound CrSi<sub>2</sub> has been the most extensively studied material since its initial characterization as an 0.35-eV band-gap semiconductor in the mid-1960s.<sup>5</sup> The analysis of subsequent transport data<sup>6</sup> has yielded a slightly smaller estimate ( $\sim 0.30$  eV) of the CrSi<sub>2</sub> band gap, along with indications of relatively large hole and electron effective-mass ratios ( $m^*/m_0 \sim 3$  and 20, respectively). Such masses seem consistent with the enhanced Cr 3*d* character near  $E_F$  that is expected for a refractory compound.

Potential optoelectronic device applications that combine semiconductor-semiconductor heterojunctions with silicon-based integrated-circuit technology have stimulated efforts to grow epitaxial CrSi<sub>2</sub> thin films on various faces of Si.<sup>7,8</sup> Despite a favorable lattice match with Si(111), these attempts have produced small grained ( $\sim 2$   $\mu\text{m}$ ) epitaxial regions that cover only a fraction ( $\sim 70\%$ ) of the total interface. A promising technique for fabricating Si/CrSi<sub>2</sub>/Si heterostructures with improved interfaces utilizes ion implantation to form thin buried layers of CrSi<sub>2</sub> in Si(111) wafers.<sup>9</sup>

At present, a detailed understanding of the nature and origin of the semiconducting gap in CrSi<sub>2</sub> is lacking. One proposal<sup>1</sup> suggests that magnetic influences may be important. Indeed, the results of a band calculation<sup>10</sup> for

hexagonal CrSi<sub>2</sub> predict semimetallic rather than semiconducting behavior. However, recent optical studies<sup>11</sup> have provided convincing evidence that a standard band-like picture is applicable. According to these measurements, CrSi<sub>2</sub> has an indirect band gap of  $\sim 0.35$  eV, with indications of strong direct transitions at slightly higher ( $\sim 0.67$  eV) energies.

These developments have stimulated the present effort to explore the applicability of a simple band picture for explaining the semiconductor gap in hexagonal CrSi<sub>2</sub>. With this objective, the linear augmented-plane-wave (LAPW) method has been applied to calculate the electronic band structure of bulk hexagonal CrSi<sub>2</sub> in the local-density approximation (LDA). The present implementation of the LAPW method<sup>12</sup> imposes no shape approximations on either the crystalline charge density or the potential. Exchange and correlation effects are treated with the use of the Wigner interpolation formula.<sup>13</sup> The present calculations include a basis of  $\sim 500$  LAPW's (12 Ry plane-wave cutoff) and spherical-harmonic terms through  $l=6$ . The crystalline charge density and potential are expanded with about 5000 plane waves (55 Ry) in the interstitial region and lattice harmonics ( $l_{\text{max}}=4$ ) within the muffin-tin spheres. A 14-point **k** mesh in the irreducible  $\frac{1}{24}$  wedge has been used to carry out Brillouin-zone integrations.

The essential features of the hexagonal *C40* structure are illustrated in Fig. 1. It consists of identical hexagonal CrSi<sub>2</sub> layers which are stacked in an *ABC* sequence such that successive layers are rotated by 60° about an origin (\*). The intralayer Cr-Si bond lengths ( $\sim 2.55$  Å) are determined by a Si-atom position parameter *x*. Total-energy calculations<sup>14</sup> show that deviations from the "ideal"  $x = \frac{1}{6}$  value<sup>15</sup> are minimal ( $\Delta x = 1.5 \times 10^{-4}$ ). The *C40* space group ( $D_6^4$ ) is nonsymmorphic, containing a screw axis that interchanges layers via the nonprimitive translations  $\tau = 0, c/3, \text{ and } 2c/3$ .  $E_{n,\mathbf{k}}$  exhibits full hexagonal ( $D_{6h}$ ) symmetry as a result of time reversal.<sup>16</sup> The orthorhombic and tetragonal phases that characterize the other refractory disilicides (see Table I) involve alternative four-layer (*ABCD* for *C54*) or two-layer (*AB'* for *C49* and *AB* for *C11<sub>b</sub>*) variations on the three-layer *ABC* stacking of the hexagonal *C40* phase.<sup>3</sup> The ubiquity of these hexagonal *RSi<sub>2</sub>* layers implies an intrinsic stability that should enhance their epitaxial growth at Si inter-

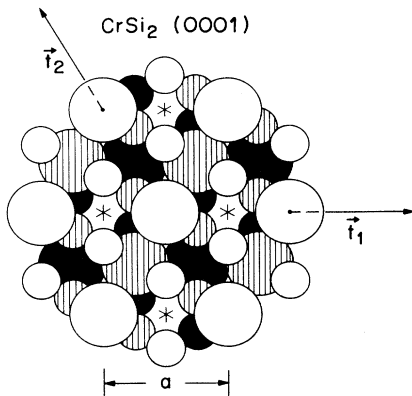


FIG. 1. Projected (0001) view of hexagonal  $C40$   $\text{CrSi}_2$  illustrating the  $ABC$  stacking of hexagonal  $\text{CrSi}_2$  layers. Cr (Si) atoms are represented by the large (small) circles; neighboring primitive-cell origins are labeled with \*'s.

faces.

Because the  $C40$  structure contains three formula units per primitive cell, a complex band structure can be anticipated for hexagonal  $\text{CrSi}_2$ . These expectations are realized in the LAPW band results which are shown in Fig. 2. As indicated by the triangle symbols, the lowest  $\text{CrSi}_2$  bands have predominant Si  $3s, 3p$  character, which then gradually switches to Cr  $3d$  character near  $E_F$ . Within this Cr  $3d$  manifold, an  $0.30\text{-eV}$  indirect band gap occurs between the highest filled valence-band state  $E_{n,k}$  at  $L$  ( $n=21$ ) and the lowest unoccupied conduction-band state at  $M$  ( $n=22$ ). This calculated LDA gap is in excellent agreement with the measured  $0.35\text{-eV}$  optical gap.<sup>11</sup> However, the calculated lowest-energy direct transition at  $L$  is somewhat smaller than the observed value ( $0.45$  vs  $0.67$  eV).

The origin of the  $\text{CrSi}_2$  band gap within the Cr  $3d$  manifold is rather complex, involving the hybridization of specific  $3d$  orbitals with the Si  $3p$  states in neighboring layers. As shown in the upper portion of Fig. 3, states near the valence-band maximum have predominant  $d_{3z^2-r^2}$  symmetry while the conduction-band minimum involves  $d_{xz, yz}$ -type states. Despite substantial  $d$  character, the calculated effective masses are close to the free-electron values for both the valence and conduction bands. Specifically, the principal-axis effective-mass ratios for

TABLE I. Observed crystal structures of the refractory transition-metal disilicides  $\text{RSi}_2$  (Ref. 2).  $O$ ,  $H$ , and  $T$  denote phases with orthorhombic, hexagonal, and tetragonal symmetry, respectively.

Series	IV	Group V	VI
$3d$	$\text{TiSi}_2$	$\text{VSi}_2$	$\text{CrSi}_2$
	$O(C54)$	$H(C40)$	$H(C40)$
$4d$	$\text{ZrSi}_2$	$\text{NbSi}_2$	$\text{MoSi}_2$
	$O(C49)$	$H(C40)$	$T(C11_b)$
$5d$	$\text{HfSi}_2$	$\text{TaSi}_2$	$\text{WSi}_2$
	$O(C49)$	$H(C40)$	$T(C11_b)$

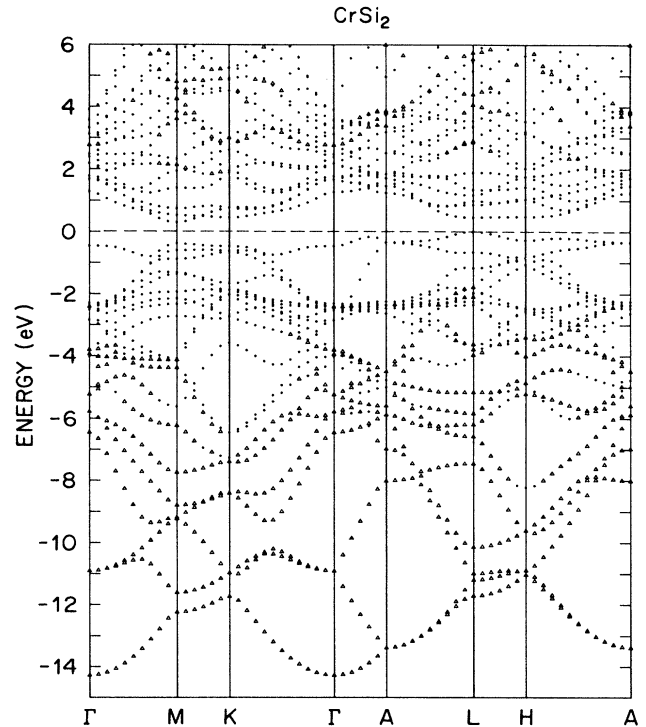


FIG. 2. LAPW energy-band results for hexagonal ( $C40$ )  $\text{CrSi}_2$ . Triangles identify bands with significant Si  $3s, 3p$  orbital weight ( $>15\%$ ) within the Si muffin-tin spheres.

holes [electrons] at  $L$  [ $M$ ] are  $(1.2, 1.3, 0.9)$  [ $0.7, 0.7, 1.4$ ]. These are significantly smaller than the corresponding experimental values of  $\sim 3$ [ $20$ ].<sup>6</sup> Clearly, independent measurements would be useful in clarifying this discrepancy.

The excellent agreement between the calculated  $\text{CrSi}_2$  band gap and experiment is unanticipated, since the LDA greatly underestimates semiconductor band gaps in many other systems. Its success in  $\text{CrSi}_2$  may be understood in terms of the analysis of the many-body self-energy operator given by Godby, Schlüter, and Sham.<sup>17</sup> They showed that the spatial nonlocality of this operator was the dominant characteristic which produced accurate band gaps. When integrated against the relatively smooth valence-band wave functions, it produced a more attractive effective potential than the more rapidly oscillating conduction-band functions.<sup>17</sup> While such qualitative differences between the valence- and conduction-band states are found in the conventional group IV and III-V semiconductors, the dominant spatial scale of nearby states on both sides of the  $\text{CrSi}_2$  band gap is the same, set by the Cr  $3d$  orbitals. As noted above, the  $\text{CrSi}_2$  gap originates from a subtle combination of hybridization and crystal-field effects which do not modify significantly the shape of the high-amplitude  $3d$  portion of these wave functions. It is, therefore, plausible that the state dependence of the self-energy should be small within this group of bands, and the band splittings accurately represented by the LDA potential.<sup>18</sup>

Because of its small value, one can expect the calculat-

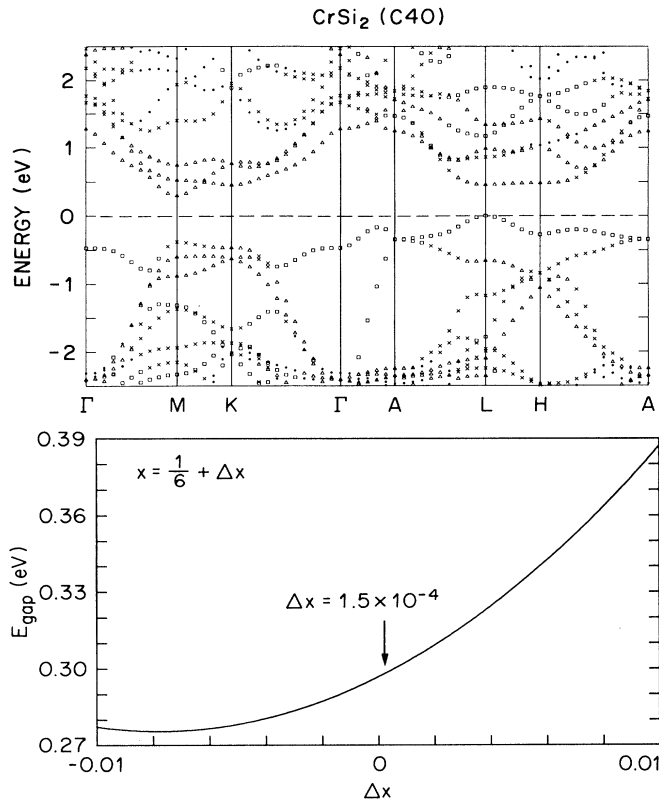


FIG. 3. LAPW energy-band results near  $E_F$  for hexagonal  $\text{CrSi}_2$ . Bands with specific  $3d$ -orbital character are distinguished by squares ( $d_{3z^2-r^2} > 15\%$ ), triangles ( $d_{xz,yz} > 30\%$ ), and  $x$ 's ( $d_{xy,x^2-y^2} > 30\%$ ). Calculated dependence of the  $\text{CrSi}_2$  band gap  $E_{\text{gap}}$  on the Si-atom position parameter  $x$ .

ed  $\text{CrSi}_2$  band gap to be sensitive to both structural and chemical changes. Substantially reduced gaps are calculated<sup>14</sup> for the metastable  $C40$  phases of  $\text{MoSi}_2$  (+0.02 eV) and  $\text{WSi}_2$  (−0.03 eV). Analogous calculations show that a 2% reduction in the  $\text{CrSi}_2$   $c$ -axis lattice parameter causes an 8-meV decrease in the band gap. The calculated gap is particularly sensitive to the Si-atom position parameter  $x$  that determines the Cr-Si coordination geometry within each  $\text{CrSi}_2$  layer. In the results presented thus far, this parameter has been fixed at its ideal  $x = \frac{1}{6}$  value, where each Si atom has six equidistant planar neighbors. The dependence of the  $\text{CrSi}_2$  band gap  $E_{\text{gap}}$  on small  $\Delta x$  variations is shown in the lower portion of Fig. 3. It is seen that  $E_{\text{gap}}$  varies by  $\sim 0.1$  eV for  $\Delta x$  changes of  $\pm 0.01$ . However, the resulting increase in the predicted  $\text{CrSi}_2$  band gap is minimal ( $\sim 1$  meV) for the calculated shift,<sup>14</sup>  $\Delta x \approx 1.5 \times 10^{-4}$ .

The effect of stacking sequence changes on the  $\text{CrSi}_2$  bands near  $E_F$  is illustrated in Fig. 4. In these calculations, lattice parameters for the tetragonal  $C11_b$  and orthorhombic  $C54$  phases have been derived from the  $C40$  values<sup>15</sup> ( $a = 4.420$  Å,  $c = 6.349$  Å) using the relations  $a_1 = \sqrt{2}a/2$ ,  $c_1 = \sqrt{3}a$ , and  $a_0 = \sqrt{3}a$ ,  $b_0 = a$ ,  $c_0 = 4c/3$ . These parameters preserve the  $C40$  intraplanar  $\text{CrSi}_2$  bond distances in both phases. Tetragonal symmetry increases the  $C40$   $\text{CrSi}_2$  interlayer separation from 2.12 to

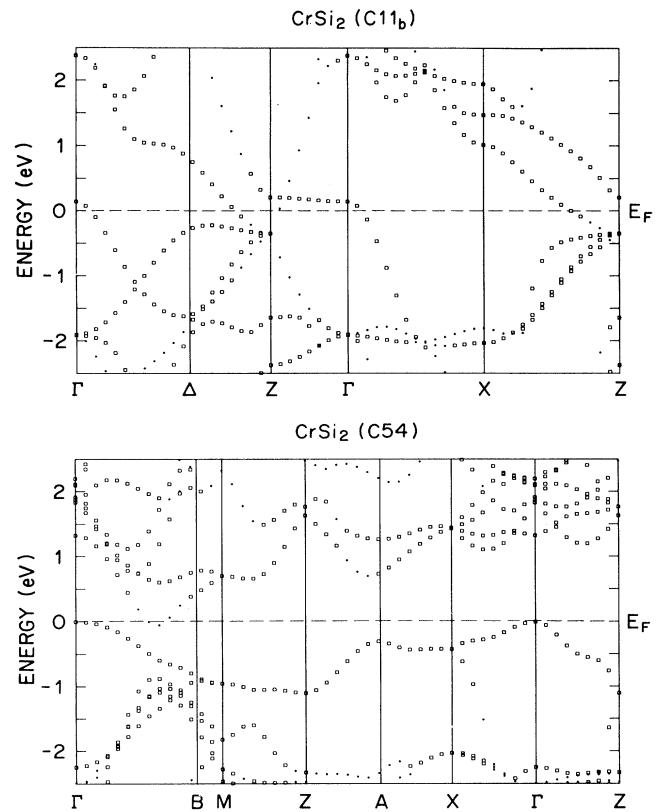


FIG. 4. Effect of alternative layer sequencing on the  $\text{CrSi}_2$  bands near  $E_F$ , including the  $AB$  and  $ABCD$  stacking of the tetragonal ( $C11_b$ ) and orthorhombic ( $C54$ ) phases. The squares identify bands with dominant Cr  $3d$  orbital character ( $d > 50\%$ ).

2.21 Å for the  $C11_b$  phase. However, the  $C40$  geometry is changed only in the fourth layer ( $\sim 8.5$  Å) in the  $C54$  calculation.

As shown by the results in Fig. 4, both hypothetical forms of  $\text{CrSi}_2$  exhibit semimetallic behavior. The tetragonal ( $C11_b$ ) results are in good agreement with those<sup>19</sup> for the isostructural compounds  $\text{MoSi}_2$  and  $\text{WSi}_2$ . In the  $C54$ -phase results, the slight ( $\sim 0.05$  eV) band overlap is the result of increased hybridization of the Cr  $3d$  states with Si  $3p$  orbitals. Thus, a subtle combination of symmetry and distant-neighbor ( $\sim 8.5$  Å) coordination changes is sufficient to eliminate the  $C40$   $\text{CrSi}_2$  band gap. The calculations show that the total energies of all three  $\text{CrSi}_2$  phases are comparable, with the  $C11_b$  ( $\sim 0.01$  eV/formula unit) and  $C54$  ( $\sim 0.1$  eV/formula unit) phases slightly less stable than  $C40$   $\text{CrSi}_2$ . This suggests the possible presence of low-energy stacking faults in thin-film  $\text{CrSi}_2$  samples, a potential detriment in device applications that exploit the semiconducting properties of bulk  $\text{CrSi}_2$ .

To summarize, band calculations confirm that hexagonal  $\text{CrSi}_2$  is a small-gap semiconductor, yielding a band gap of 0.30 eV which is in excellent agreement with experiment. This calculated gap is sensitive to subtle structural-symmetry variations that transform the  $C40$  phase into the closely related  $C54$  and  $C11_b$  structures.

I am pleased to acknowledge several useful discussions with D. R. Hamann during the course of this investigation.

- 
- <sup>1</sup>S. P. Murarka, *J. Vac. Sci. Technol.* **17**, 775 (1980).  
<sup>2</sup>M.-A. Nicolet and S. S. Lau, in *VLSI Electronics: Microstructure Science*, Vol. 6, edited by N. G. Einspruch and G. B. Larrabee (Academic, New York, 1983), p. 329.  
<sup>3</sup>F. Laves, in *Theory of Alloy Phases* (American Society for Metals, Metal Park, Cleveland, OH, 1956), p. 181.  
<sup>4</sup>J. H. Weaver, A. Franciosi, and V. L. Moruzzi, *Phys. Rev. B* **29**, 3293 (1984).  
<sup>5</sup>D. Shinoda, S. Asanabe, and Y. Sasaki, *J. Phys. Soc. Jpn.* **19**, 269 (1964).  
<sup>6</sup>I. Nishida and T. Sakata, *J. Phys. Chem. Solids* **39**, 499 (1978).  
<sup>7</sup>F. Y. Shiau, H. C. Cheng, and L. J. Chen, *Appl. Phys. Lett.* **45**, 524 (1984); *J. Appl. Phys.* **59**, 2784 (1986).  
<sup>8</sup>R. W. Fathauer, P. J. Grunthaner, T. L. Lin, K. T. Chang, J. H. Mazur, and D. N. Jamieson, *J. Vac. Sci. Technol. B* **6**, 708 (1988).  
<sup>9</sup>A. E. White, K. T. Short, and D. J. Eaglesham, *Appl. Phys. Lett.* **56**, 1260 (1990).  
<sup>10</sup>A. Franciosi, J. H. Weaver, D. G. O'Neill, F. A. Schmidt, O. Bisi, and C. Calandra, *Phys. Rev. B* **28**, 7000 (1983).  
<sup>11</sup>M. C. Bost and J. E. Mahan, *J. Appl. Phys.* **63**, 839 (1988).  
<sup>12</sup>L. F. Mattheiss and D. R. Hamann, *Phys. Rev. B* **33**, 823 (1986).  
<sup>13</sup>E. Wigner, *Phys. Rev.* **46**, 1002 (1934).  
<sup>14</sup>Details will be provided in a separate publication.  
<sup>15</sup>W. B. Pearson, *A Handbook of Lattice Spacings and Structures of Metals and Alloys* (Pergamon, New York, 1958).  
<sup>16</sup>M. Lax, *Symmetry Principles in Solid State and Molecular Physics* (Wiley, New York, 1974).  
<sup>17</sup>R. W. Godby, M. Schlüter, and L. J. Sham, *Phys. Rev. Lett.* **56**, 2415 (1986); *Phys. Rev. B* **36**, 6497 (1987).  
<sup>18</sup>R. O. Jones and O. Gunnarsson, *Phys. Rev. Lett.* **55**, 107 (1985).  
<sup>19</sup>B. K. Bhattacharyya, D. M. Bylander, and L. Kleinman, *Phys. Rev. B* **32**, 7973 (1985).